

# Topology optimization in Bernoulli free boundary problems\*

J. I. Toivanen<sup>†</sup> R.A.E. Mäkinen<sup>‡</sup> J. Haslinger<sup>§</sup>

January 15, 2021

## Abstract

In this work we consider topology optimization of systems, which are governed by the external Bernoulli free boundary problem. We utilize the so-called pseudo-solid approach to solve the governing free boundary problems during the optimization. To define design domains we utilize a level set representation parameterized by radial basis functions. This design parametrization allows topological changes in the design domain.

## Introduction

In shape optimization, state problems are usually given by partial differential equations which are formulated and solved in known domains. Thus the unknown shape we are looking for is represented by a solution to our optimization problem. If the state is defined by a free boundary problem, the situation becomes more involved. The main feature of such problems is the fact that not only a function solving the respective PDE but also the domain itself where this PDE is considered are unknown and they have to be found simultaneously. Unlike to the standard case, the unknown geometry now appears in both, the upper as well as the inner level of the optimization problem. Classical shape optimization with external Bernoulli free boundary problems (BFBP) as the state relation has been presented in [1]. A couple  $(u, \Omega)$  is said to be a solution to BFBP if  $u$  is harmonic in a doubly connected (unknown) domain  $\Omega$ , it satisfies the Dirichlet condition on the boundary  $\partial\omega$  of the inner component  $\omega$  given a-priori and, in addition the over-determined system consisting of the Neumann and Dirichlet condition on the (unknown) free boundary. The shape of the free boundary was controlled by  $\omega$  but still keeping the same topology of  $\omega$ . To make numerical realization simpler we supposed that the system of admissible  $\omega$ :s consists of star-like domains enabling us to express  $\partial\omega$  and  $\omega$  in terms of the polar coordinates. However it was observed that this system is very narrow and many reasonable target free boundaries can not be matched. Indeed, if the boundary  $\partial\omega$  is twice differentiable and  $\omega$  is star-like with respect to a neighborhood of some point in  $\omega$  then the respective free boundary is of the class  $C^\infty$  [2]. Hence if a given target free boundary has the discontinuous curvature (a square with rounded corners, e.g) then it can never be realized for any such  $\omega$ . In computations this fact manifests

---

\*The research of the second author was supported by the grant #122932 of the Academy of Finland. The third author acknowledges the support of the grant IAA100750802 of the Grant Agency of the Czech Academy of Science and MSM0021620839.

<sup>†</sup>Department of Mathematical Information Technology, University of Jyväskylä, PO Box 35 (Agora), 40014 Jyväskylä, Finland

<sup>‡</sup>Department of Mathematical Information Technology, University of Jyväskylä, PO Box 35 (Agora), 40014 Jyväskylä, Finland

<sup>§</sup>Faculty of Mathematics and Physics, Department of Numerical Mathematics, Charles University Prague, Sokolovska 83, 186 75, Prague 8, Czech Republic

itself by oscillations of  $\partial\omega$ : using finer discretizations of  $\partial\omega$ , the oscillations become faster and faster (see [1]). This behavior indicates the tendency to change the topology of  $\omega$ . There are two ways how to overcome such oscillations: i) to restrict the design space ii) to extend it in such a way that changes of topology are possible. If i) is used then oscillations are suppressed but usually there is a big gap between the target and the found free boundary. To get better results one has to change the topology of  $\omega$ . One of possible ways how to do that will be described in this paper. We shall use a level set approach. The topology of  $\omega$  will be determined by the zero level set of a function whose argument is given by the linear combination of a system of radial basis functions with overlapping supports. Instead of solving Hamilton-Jacobi equation describing the evolution of the level set function, the problem can be treated as a parametric minimization problem with parameters represented by the coefficients of the above mentioned linear combination.

The paper is organized as follows: Section 1 presents a general setting of a class of topology optimization problems governed by BFBP. Section 2 is devoted to the presentation of the state solver. Since the state problem will be solved several times, one has to have at his disposal an efficient and reliable method. It turns out that the so-called pseudo-solid approach enjoys both these requirements. In Section 3 we shortly recall a level set approach widely used in topology optimization. Section 4 deals with a discretization of the whole optimization problem and its numerical realization when  $C^2$  radial basis functions are used to parameterize the level set function. Section 5 presents results of several model examples. Finally, the paper is completed with two appendices on smoothing the Heaviside function and on the analytical solution to a specific Bernoulli problem.

Throughout the paper we use the following notation: the symbol  $H^k(\Omega)$  ( $k \geq 0$  integer) stands for the Sobolev space of functions which are together with their derivatives up to order  $k$  square integrable in  $\Omega$ , i.e. elements of  $L^2(\Omega)$  (we set  $H^0(\Omega) \equiv L^2(\Omega)$ ).

## 1 Setting of the problem

We start with the definition of the state problem represented by an exterior Bernoulli free boundary problem. Let  $\gamma < 0$  and an open set  $\omega \subset \mathbb{R}^2$  with a sufficiently regular boundary  $\partial\omega$  be given. The problem consists in finding a set  $\Omega \supset \bar{\omega}$  and a function  $u : \Omega \setminus \bar{\omega} \rightarrow \mathbb{R}$  satisfying

$$\left\{ \begin{array}{l} \Delta u = 0 \quad \text{in } \Omega \setminus \bar{\omega} \\ u = 1 \quad \text{on } \partial\omega \\ u = 0 \\ \frac{\partial u}{\partial \mathbf{n}} = \gamma \end{array} \right\} \quad \text{on } \partial\Omega. \quad (\tilde{\mathcal{P}}(\omega))$$

This paper deals with the control of the shape of  $\Omega$  in  $(\tilde{\mathcal{P}}(\omega))$ . The geometry of the free boundary  $\partial\Omega$  will be driven by the shape of  $\omega$  towards a given target free boundary  $\Gamma_t$ . Our optimization problem reads as follows:

$$\left\{ \begin{array}{l} \text{Find } \omega^* \in \tilde{\mathcal{O}} \text{ such that} \\ J(\Gamma(\omega^*)) \leq J(\Gamma(\omega)) \end{array} \right. \quad (\tilde{\mathcal{P}})$$

holds for any  $\omega \in \tilde{\mathcal{O}}$ , where  $\tilde{\mathcal{O}}$  is a set of admissible designs. The cost functional to be considered is the distance between  $\Gamma_t$  and the free boundary  $\Gamma(\omega) := \partial\Omega(\omega)$  being the solution of  $(\tilde{\mathcal{P}}(\omega))$ , i.e.

$$J(\Gamma(\omega)) = \rho(\Gamma(\omega), \Gamma_t), \quad (1)$$

where  $\rho$  is a function characterizing the distance of  $\Gamma(\omega)$  from  $\Gamma_t$ .

In this paper we make the assumption that  $\Omega$  is a *star-like domain*. However, in contrast to [1] no such assumption is made on  $\omega$  meaning that also the topology of  $\omega$  may change.

## 2 Pseudo-solid formulation of Bernoulli free boundary problems

Free boundary problems have in common the difficulty that the geometry (here the domain  $\Omega$ ) has to be determined simultaneously with the solution  $u$  of the state problem, which implies that a numerical solution has to be done iteratively [3]. Possible solution strategies include trial methods, linearization methods (continuous or discrete) [4], and shape optimization methods [5]. We decided for the so-called *pseudo-solid approach* (PSA) in which the unknown domain  $\Omega$  is obtained by an appropriate deformation of the reference configuration  $\widehat{\Omega}$ . This deformation is one of the unknowns in PSA. The main advantage of this approach is that there is no need to construct an explicit parametrization of the geometry using e.g. a conformal mapping of the reference domain. PSA is useful also in numerical realization: finite element partitions of  $\Omega$  can be constructed via the respective deformation of the partition of  $\widehat{\Omega}$ . As the Bernoulli problem has to be solved several times for different  $\omega$ , the choice of an efficient solver is also important. We use Newton's method because of its fast convergence. Moreover, this solution strategy readily allows us to obtain geometrical sensitivities of the system.

Let  $\widehat{\Omega} \subset \mathbb{R}^2$  be a fixed, simply connected reference domain. In the pseudo-solid technique we construct a mapping  $F : \mathbb{R}^2 \rightarrow \mathbb{R}^2$ ,  $\widehat{\Omega} \mapsto F(\widehat{\Omega}) =: \Omega$  such that  $\Omega$  solves  $(\widetilde{\mathcal{P}}(\omega))$  for given  $\omega$ . To construct such  $F$  we treat  $\widehat{\Omega}$  as an elastic solid that undergoes a deformation caused by an external loading  $p$  such that the deformed solid defines such  $\Omega$ . Thus, problem  $(\widetilde{\mathcal{P}}(\omega))$  is strongly coupled with the Lamé system of linear elasticity in which the loading  $p$  applied to  $\partial\widehat{\Omega}$  plays the role of an unknown in PSA. This approach has been previously used to solve free surface flow problems (see e.g. [6, 7]) and Bernoulli free boundary problems in [1].

For any  $\mathbf{w} \in W^{ad} := \{\text{"sufficiently" small and regular deformations}\}$  we define the domain

$$\Omega_{\mathbf{w}} = \{\mathbf{x} \in \mathbb{R}^2 \mid \mathbf{x} = \widehat{\mathbf{x}} + \mathbf{w}(\widehat{\mathbf{x}}), \quad \widehat{\mathbf{x}} \in \widehat{\Omega}\}.$$

We introduce the following function spaces:

$$\begin{aligned} W_{\omega} &= \{\mathbf{w} \in [H^1(\widehat{\Omega})]^2 \mid \mathbf{w}|_{\omega} = \mathbf{0}\} \\ V_c(\Omega) &= \{\varphi \in H^1(\Omega) \mid \varphi|_{\omega} = c\}, \quad c \in \mathbb{R}. \end{aligned}$$

The pseudo-solid formulation of our free boundary problem then reads as follows: Given  $\omega$ , find  $(u, p, \mathbf{v}) \in V_1(\Omega_{\mathbf{v}}) \times L^2(\partial\widehat{\Omega}) \times W_{\omega}$  such that

$$\left\{ \begin{array}{l} \int_{\Omega_{\mathbf{v}} \setminus \omega} \nabla u \cdot \nabla \varphi \, d\mathbf{x} = \gamma \int_{\partial\Omega_{\mathbf{v}}} \varphi \, ds \quad \forall \varphi \in V_0(\Omega_{\mathbf{v}}) \\ \int_{\partial\Omega_{\mathbf{v}}} u \psi \, ds = 0 \quad \forall \psi \in L^2(\partial\Omega_{\mathbf{v}}) \\ \int_{\widehat{\Omega} \setminus \omega} \sigma(\mathbf{v}) : \varepsilon(\mathbf{w}) \, d\mathbf{x} = \int_{\partial\widehat{\Omega}} p \mathbf{n} \cdot \mathbf{w} \, ds \quad \forall \mathbf{w} \in W_{\omega}. \end{array} \right. \quad (\mathcal{P}(\omega))$$

Equations  $(\mathcal{P}(\omega)_1)$  and  $(\mathcal{P}(\omega)_2)$  constitute the weak form of  $(\widetilde{\mathcal{P}}(\omega))$  while  $(\mathcal{P}(\omega)_3)$  is the weak form of the linear elasticity problem in  $\widehat{\Omega} \setminus \omega$ . Here  $p\mathbf{n}$  is an (unknown) external load. The components of the strain and stress tensors  $\varepsilon = \{\varepsilon_{ij}(\mathbf{v})\}$  and  $\sigma = \{\sigma_{ij}(\mathbf{v})\}$  associated with a displacement field  $\mathbf{v}$  are given by

$$\varepsilon_{ij}(\mathbf{v}) = \frac{1}{2} \left( \frac{\partial v_i}{\partial x_j} + \frac{\partial v_j}{\partial x_i} \right), \quad \sigma_{ij}(\mathbf{v}) = 2\mu \varepsilon_{ij}(\mathbf{v}) + \lambda \delta_{ij} \nabla \cdot \mathbf{v}, \quad i, j = 1, 2,$$

respectively, where  $\mu$  and  $\lambda$  are the Lamé coefficients. Since in this case the linear elasticity system does not have any physical meaning, the Lamé coefficients can be chosen quite freely. In this paper the choice  $\mu = 0.5$  and  $\lambda = 0$  was made. The solvability of  $(\mathcal{P}(\omega))$  is analyzed in details in [1]. The relation between  $(\tilde{\mathcal{P}}(\omega))$  and  $(\mathcal{P}(\omega))$  is readily seen: if  $(u, p, \mathbf{v})$  is a solution of  $(\mathcal{P}(\omega))$  then the couple  $(u|_{\Omega_v \setminus \bar{\omega}}, \Omega_v)$  solves  $(\tilde{\mathcal{P}}(\omega))$ .

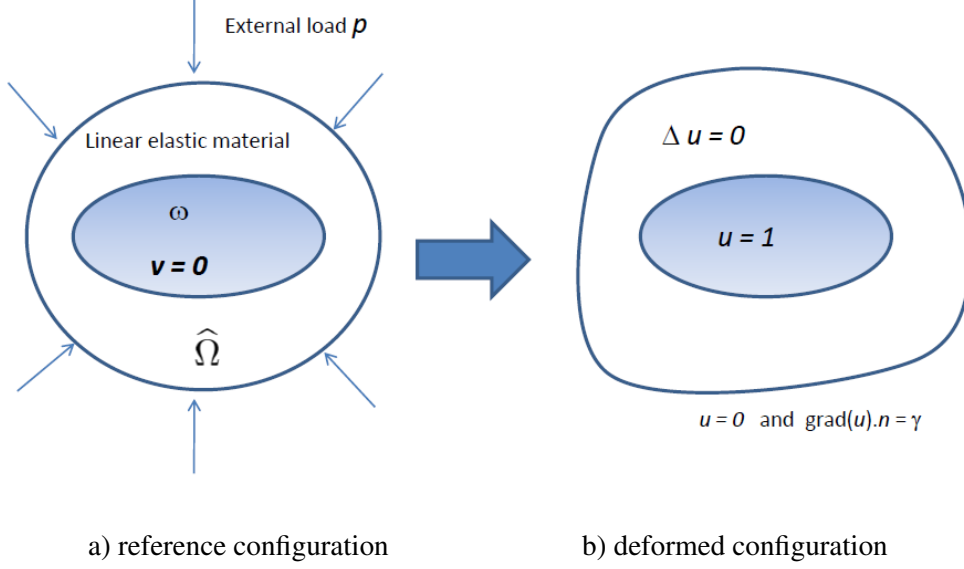


Figure 1: Principle of the pseudo-solid approach.

### 3 Level set approach to the optimization problem

In the previous paper [1] the design domain  $\omega$  was parameterized using the polar co-ordinates. A tendency towards fractal-like designs indicating possible topological changes of  $\omega$  was observed in certain cases. However, the boundary variation technique used in [1] is not able to handle topological changes automatically. This will be done by a level set parametrization [8, 9] of  $\omega$ .

The basic idea is simple: Let  $D$  be a larger domain containing all admissible  $\omega$  (for example a rectangle slightly larger than the bounding box of the target boundary  $\Gamma_t$ ). Let  $\psi : D \rightarrow \mathbb{R}$  be given and define the set  $\omega$  by

$$\omega := \omega(\psi) := \{\mathbf{x} \in D \mid \psi(\mathbf{x}) > 0\}, \quad \psi \in U^{ad}. \quad (2)$$

Here  $U^{ad}$  is a family of admissible level set functions such that  $\psi \in U^{ad} \implies \omega(\psi) \in \tilde{\mathcal{O}}$ . Clearly the parametrization (2) allows topological changes of  $\omega$ .

We can now reformulate problem  $(\hat{\mathbb{P}})$  as follows:

$$\begin{cases} \text{Find } \psi^* \in U^{ad} \text{ such that} \\ J(\Gamma(\psi^*)) \leq J(\Gamma(\psi)) \quad \forall \psi \in U^{ad}, \end{cases} \quad (\hat{\mathbb{P}})$$

where  $\Gamma(\psi)$  is the free boundary defined by  $(\mathcal{P}(\omega(\psi)))$

Next we introduce the following relaxed state problem which does not contain explicitly any Dirichlet type boundary conditions. For  $\varepsilon > 0$ ,  $\psi \in U^{ad}$  given:

Find  $(u_\varepsilon, p_\varepsilon, \mathbf{v}_\varepsilon) \in H^1(\Omega_{\mathbf{v}_\varepsilon}) \times L^2(\partial\widehat{\Omega}) \times [H^1(\widehat{\Omega})]^2$  such that

$$\left\{ \begin{array}{l} \int_{\Omega_{\mathbf{v}_\varepsilon}} \nabla u_\varepsilon \cdot \nabla \varphi \, d\mathbf{x} - \gamma \int_{\partial\Omega_{\mathbf{v}_\varepsilon}} \varphi \, ds + \int_{\Omega_{\mathbf{v}_\varepsilon}} G_\varepsilon(\psi)(u_\varepsilon - 1)\varphi \, d\mathbf{x} = 0 \quad \forall \varphi \in H^1(\Omega_{\mathbf{v}_\varepsilon}) \\ \int_{\partial\Omega_{\mathbf{v}_\varepsilon}} u_\varepsilon \psi \, ds = 0 \quad \forall \psi \in L^2(\partial\Omega_{\mathbf{v}_\varepsilon}) \\ \int_{\widehat{\Omega}} \sigma(\mathbf{v}_\varepsilon) : \varepsilon(\mathbf{w}) \, d\mathbf{x} - \int_{\partial\widehat{\Omega}} p_\varepsilon \mathbf{n} \cdot \mathbf{w} \, ds + \int_{\widehat{\Omega}} G_\varepsilon(\psi) \mathbf{v}_\varepsilon \cdot \mathbf{w} \, d\mathbf{x} = 0 \quad \forall \mathbf{w} \in [H^1(\widehat{\Omega})]^2. \end{array} \right. \quad (\mathcal{P}_\varepsilon(\psi))$$

Above,  $G_\varepsilon$  is a penalty function releasing the constraints  $u = 0$  and  $\mathbf{v} = \mathbf{0}$  in  $\omega$ . The classical choice is  $G_\varepsilon = \frac{1}{\varepsilon}H$ , where  $H$  is the Heaviside function. This choice of  $G_\varepsilon$  will be used in what follows.

We define now the ‘‘relaxed’’ optimization problem

$$\left\{ \begin{array}{l} \text{Find } \psi_\varepsilon^* \in U^{ad} \text{ such that} \\ J(\Gamma_\varepsilon(\psi_\varepsilon^*)) \leq J(\Gamma_\varepsilon(\psi)) \quad \forall \psi \in U^{ad}, \end{array} \right. \quad (\mathbb{P}_\varepsilon)$$

where  $\Gamma_\varepsilon(\psi) = F_\varepsilon(\partial\widehat{\Omega})$ ,  $F_\varepsilon = \text{id} + \mathbf{v}_\varepsilon$  and  $\mathbf{v}_\varepsilon$  is the third component of the solution of  $(\mathcal{P}_\varepsilon(\psi))$ .

## 4 Discretization

One of the advantages of level set methods is that they avoid tracking of the boundary of the design domain. Instead a fixed mesh is used. In our case the mesh  $\widehat{\mathcal{T}}$  of the reference domain  $\widehat{\Omega}$  is fixed, but the mesh  $\mathcal{T}$  of  $\Omega$  is moving according to the pseudo-solid strategy. However, the boundary of  $\omega$  is not exactly tracked in either of these meshes. An unstructured mesh consisting of triangles is used to approximate  $\widehat{\Omega}$ . The mesh of  $\Omega_{\mathbf{v}}$  is obtained by displacing the nodes of  $\widehat{\mathcal{T}}$  using the discrete displacement field  $\mathbf{v}_h$  which approximates  $\mathbf{v}$ .

### 4.1 Discretization of the state problem

Let  $\varepsilon > 0$ ,  $\psi \in U^{ad}$  be given. To simplify notation, the penalty parameter  $\varepsilon$  at the discrete solution will be omitted. The finite element discretization of  $(\mathcal{P}_\varepsilon(\psi))$  reads as follows:

Find  $(u_h, p_h, \mathbf{v}_h) \in V_h(\Omega_{\mathbf{v}_h}) \times Q_h \times \mathbf{W}_h$  such that

$$\left\{ \begin{array}{l} \int_{\Omega_{\mathbf{v}_h}} \nabla u_h \cdot \nabla \varphi_h \, d\mathbf{x} - \gamma \int_{\partial\Omega_{\mathbf{v}_h}} \varphi_h \, ds + \int_{\Omega_{\mathbf{v}_h}} G_\varepsilon(\psi)(u_h - 1)\varphi_h \, d\mathbf{x} = 0 \quad \forall \varphi_h \in V_h(\Omega_{\mathbf{v}_h}) \\ \int_{\partial\Omega_{\mathbf{v}_h}} u_h \mu_h \, ds = 0 \quad \forall \mu_h \in Q_h(\partial\Omega_{\mathbf{v}_h}) := V_h(\Omega_{\mathbf{v}_h})|_{\partial\Omega_{\mathbf{v}_h}} \\ \int_{\widehat{\Omega}} \sigma(\mathbf{v}_h) : \varepsilon(\mathbf{w}_h) \, d\mathbf{x} - \int_{\partial\widehat{\Omega}} p_h \mathbf{n} \cdot \mathbf{w}_h \, ds + \int_{\widehat{\Omega}} G_\varepsilon(\psi) \mathbf{v}_h \cdot \mathbf{w}_h \, d\mathbf{x} = 0 \quad \forall \mathbf{w}_h \in \mathbf{W}_h, \end{array} \right. \quad (\mathcal{P}_\varepsilon^h(\psi))$$

where  $V_h(\Omega_{\mathbf{v}_h})$ ,  $\mathbf{W}_h = W_h \times W_h$ ,  $Q_h$  are finite element approximations of  $H^1(\Omega_{\mathbf{v}})$ ,  $[H^1(\widehat{\Omega})]^2$  and  $L^2(\partial\widehat{\Omega})$  respectively. Here we shall use linear triangular elements for constructing  $V_h(\Omega_{\mathbf{v}_h})$  and  $W_h$ , while  $Q_h = W_h|_{\partial\widehat{\Omega}}$ .

## 4.2 Discrete optimization problem

In the traditional level set method the function  $\psi$  is taken to be a function of pseudo-time  $t$ ,  $\psi := \psi(\mathbf{x}, t)$ , and the optimization process is realized by solving the Hamilton-Jacobi equation

$$\frac{\partial \psi}{\partial t} + v_n \|\nabla \psi\| = 0. \quad (3)$$

Here  $v_n$  is the velocity derived by the means of sensitivity analysis, often done on the continuous level. The function  $\psi$  is then advanced towards the steady state in pseudo-time, see e.g. [10].

Despite of the conceptual simplicity it is not so straightforward to implement the conventional level set method due to the need of appropriate upwind schemes, an extension of the velocities and re-initialization algorithms. Indeed, since the Hamilton-Jacobi equation does not in general admit a smooth solution, an appropriate upwind scheme must be used for the time integration. The velocity  $v_n$  is often meaningful only on the boundary  $\partial\omega$ , and must be extended to the whole domain, or at least into a neighborhood of  $\partial\omega$ . Finally, the function  $\psi$  should be an approximation of the signed distance function, i.e.  $\psi(\mathbf{x}) \approx \text{sign}(\psi(\mathbf{x}))\|\mathbf{x} - \mathbf{x}_0\|$ , where  $\mathbf{x}_0$  is the closest point to  $\mathbf{x}$  for which  $\psi(\mathbf{x}_0) = 0$ . To force this property a re-initialization procedure is often used.

Several approaches to overcome these difficulties have been proposed. In [11] radial basis functions (RBF) are used to define the function  $\psi$ , and the Hamilton-Jacobi equation is transformed into a system of ordinary differential equations. In [12] the function  $\psi$  is constructed combining parameterized primitives with a radial basis function representation of the so called R-functions. In [13], [14] the function  $\psi$  is approximated by the same shape functions on the same mesh used to solve the state problem. In this paper we follow [15] and utilize the compactly supported  $C^2$ -continuous radial basis functions [16] to parameterize explicitly the level set function. Then the geometry will inherit smoothness properties of the underlying parameterization. Moreover, we have a fixed set of design variables, and one can use sophisticated optimization methods instead of performing integration in the pseudo-time.

We introduce a set of  $N \times N$  basis functions, whose knots are placed in the interior of the domain  $D$  as follows. The coordinates of the knot  $(i, j)$  are given by

$$x_{ij} = x_{min} + (j - 1) \frac{x_{max} - x_{min}}{N - 1}, \quad i, j = 1, \dots, N \quad (4)$$

$$y_{ij} = y_{min} + (i - 1) \frac{y_{max} - y_{min}}{N - 1}, \quad i, j = 1, \dots, N \quad (5)$$

where  $x_{min}$  and  $x_{max}$  are the minimal and maximal  $x$ -coordinates of the rectangle  $D$ , respectively and similarly  $y_{min}$  and  $y_{max}$ . The RBF associated with this knot is then

$$\psi_{ij}(r_{ij}) = \max \{0, (1 - r_{ij})\}^4 (4r_{ij} + 1), \quad (6)$$

where

$$r_{ij} = \frac{\sqrt{(x - x_{ij})^2 + (y - y_{ij})^2}}{r_s}. \quad (7)$$

Here  $r_s > 0$  is a given parameter, the radius of the support (see Figure 2). To guarantee the overlapping of the supports of  $\psi_{ij}$  we define this parameter as

$$r_s = 4 \cdot \max \left( \frac{x_{max} - x_{min}}{N - 1}, \frac{y_{max} - y_{min}}{N - 1} \right). \quad (8)$$

The level set function  $\psi$  is then approximated by the linear combination of  $\psi_{ij}$ :

$$\psi := \psi_N(\boldsymbol{\alpha}) = \sum_{i,j=1}^N \alpha_{ij} \psi_{ij}. \quad (9)$$

Thus, the discrete design variables of the parameterized optimization problem are represented by the vector  $\boldsymbol{\alpha} = (\alpha_{11}, \alpha_{12}, \dots, \alpha_{NN})$ .

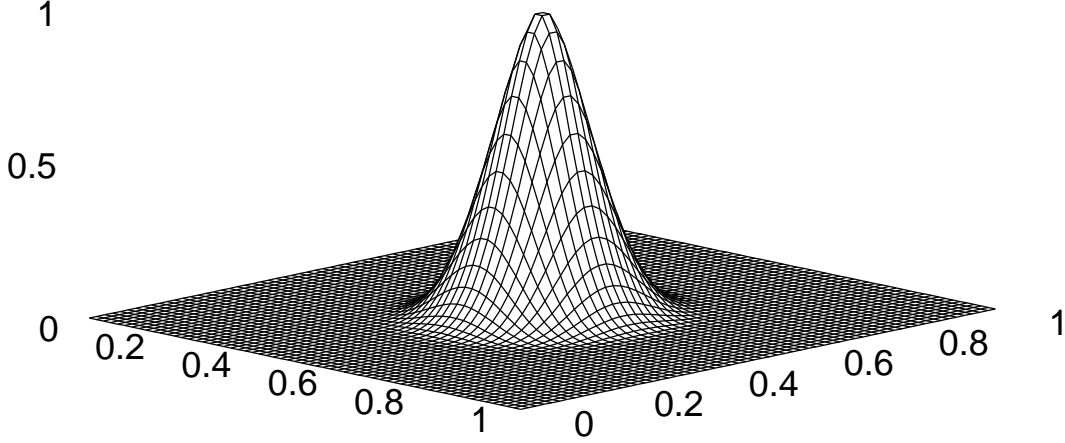


Figure 2: Surface plot of a radial basis function  $\psi_{ij}$

Using the assumption that  $\Omega$  is a star-like domain, the objective functional (1) will be given in the discrete setting by

$$\mathcal{J}(\boldsymbol{\alpha}) := J(\mathbf{v}_h(\boldsymbol{\alpha})) = \int_0^{2\pi} (g_{\boldsymbol{\alpha}}(\theta) - g_t(\theta))^2 d\theta, \quad (10)$$

where  $\boldsymbol{\alpha}$  is the vector of the discrete design variables,  $\mathbf{v}_h(\boldsymbol{\alpha})$  is a part of the solution to  $(\mathcal{P}_{\varepsilon}^h(\psi_N(\boldsymbol{\alpha})))$ ,  $g_{\boldsymbol{\alpha}}(\theta)$  is the radius of the free boundary corresponding to  $\boldsymbol{\alpha}$ , and  $g_t(\theta)$  is the radius of the target boundary at the angle  $\theta$ . The set  $U^{ad}$  of all admissible level set functions is represented by functions of the form (9) with  $\boldsymbol{\alpha} \in \mathcal{U} := [\alpha_{\min}, \alpha_{\max}]^{N \times N} \subset \mathbb{R}^{N \times N}$ , with  $\alpha_{\min}, \alpha_{\max}$  given.

Thus, the finite-dimensional optimization problem to be realized reads as follows:

$$\begin{cases} \text{Find } \boldsymbol{\alpha}^* \in \mathcal{U} & \text{such that} \\ \mathcal{J}(\boldsymbol{\alpha}^*) \leq \mathcal{J}(\boldsymbol{\alpha}) & \forall \boldsymbol{\alpha} \in \mathcal{U} \end{cases} \quad (11)$$

subject to  $(\mathcal{P}_{\varepsilon}^h(\psi_N(\boldsymbol{\alpha})))$ .

### 4.3 Construction of the initial guess

Obviously, the location of the free boundary corresponding to a given inner boundary  $\partial\omega$  is not known a priori. Therefore we start the optimization from a simple configuration where the location of the free boundary corresponding to the initial  $\omega$  is known.

Our initial guess of  $\boldsymbol{\alpha}$  is constructed in such a way that

$$\psi_N(x_{ij}, y_{ij}) = \hat{\psi}_1(x_{ij}, y_{ij}) \quad \forall i, j = 1, \dots, N \quad (12)$$

where  $(x_{ij}, y_{ij})$  are the knots of the radial basis functions and  $\hat{\psi}_1$  is given by (43) in Appendix 2 with  $R = 1$ . We obtain a system of linear equations, which is known to be invertible. The initial values for the design vector  $\alpha$  are solutions to (12). The zero level set of such function  $\psi$  then approximates  $\partial B(0, 1)$ .

For given  $\gamma$ , the initial reference domain  $\hat{\Omega}$  is taken to be the circle  $B(0, C(1, \gamma))$  (for the definition of  $C(1, \gamma)$  see Appendix 2).

#### 4.4 Algebraic form and Sensitivity analysis

Let  $\psi \in U_{ad}$  be given. In the pseudo-solid approach we simultaneously seek the scalar function  $u$ , the pressure  $p$ , and the deformation field  $\mathbf{v}$  which deforms the reference domain  $\hat{\Omega}$  into the one that solves  $(\tilde{\mathcal{P}}(\omega))$ . The elasticity system  $(\mathcal{P}_\varepsilon^h(\psi))_3$  is thus solved in the undeformed configuration  $\hat{\Omega}$  of the pseudo-solid, whereas equations  $(\mathcal{P}_\varepsilon^h(\psi))_1$  and  $(\mathcal{P}_\varepsilon^h(\psi))_2$  are solved in the deformed one. Therefore, they have to be discretized by different meshes, too. Let us denote the nodal co-ordinates of the triangulation  $\hat{\mathcal{T}}$  of  $\hat{\Omega}$  by  $\hat{\mathbf{X}}$ . We simply transform this triangulation into the one of  $\Omega_{v_h}$  which is characterized by the nodes  $\mathbf{X} = F_h(\hat{\mathbf{X}})$ , where  $F_h$  is defined by the discrete displacement field  $\mathbf{v}_h$  being the approximation of  $\mathbf{v}$ , i.e.

$$\mathbf{X} = \hat{\mathbf{X}} + \mathbf{v}_h(\hat{\mathbf{X}}). \quad (13)$$

The algebraic form of  $(\mathcal{P}_\varepsilon^h(\psi))_1$ ,  $(\mathcal{P}_\varepsilon^h(\psi))_2$  resulting from an appropriate discretization can be written as  $\mathbf{r}_1(\mathbf{q}_u, \mathbf{q}_v) = \mathbf{0}$ ,  $\mathbf{r}_2(\mathbf{q}_u, \mathbf{q}_v) = \mathbf{0}$ , respectively and the linear elasticity system  $(\mathcal{P}_\varepsilon^h(\psi))_3$  as  $\mathbf{r}_3(\mathbf{q}_v, \mathbf{q}_p) = \mathbf{0}$ , where  $\mathbf{q}_u$ ,  $\mathbf{q}_v$  and  $\mathbf{q}_p$  are the nodal values of  $u_h$ ,  $\mathbf{v}_h$  and  $p_h$ , respectively. Here the dependence of  $\mathbf{r}_1$  and  $\mathbf{r}_2$  on  $\mathbf{q}_v$  is through the nodal co-ordinates, as specified by (13). Dimensions of the vectors  $\mathbf{q}_u$ ,  $\mathbf{q}_v$  and  $\mathbf{q}_p$  are  $n$ ,  $2n$  and  $n_e$  respectively, where  $n$  is the number of the nodes in  $\hat{\mathcal{T}}$  and  $n_e$  is the number of the nodes on  $\partial\hat{\Omega}$ .

Let us introduce the following notation:

$$\mathbf{q} = \begin{bmatrix} \mathbf{q}_u \\ \mathbf{q}_v \\ \mathbf{q}_p \end{bmatrix} \quad \text{and} \quad \mathbf{r} = \begin{bmatrix} \mathbf{r}_1 \\ \mathbf{r}_2 \\ \mathbf{r}_3 \end{bmatrix}. \quad (14)$$

Then the algebraic form of the discretized coupled system  $(\mathcal{P}_\varepsilon^h(\psi))$  can be written in short as  $\mathbf{r}(\mathbf{q}) = \mathbf{0}$ . This system will be solved using Newton's method:

$$\mathbf{q}^{(k+1)} = \mathbf{q}^{(k)} - \left( \frac{\partial \mathbf{r}(\mathbf{q}^{(k)})}{\partial \mathbf{q}} \right)^{-1} \mathbf{r}(\mathbf{q}^{(k)}) \quad (15)$$

with the Jacobian matrix

$$\left( \frac{\partial \mathbf{r}}{\partial \mathbf{q}} \right) = \begin{bmatrix} \frac{\partial \mathbf{r}_1}{\partial \mathbf{q}_u} & \frac{\partial \mathbf{r}_1}{\partial \mathbf{q}_v} & \mathbf{0} \\ \frac{\partial \mathbf{r}_2}{\partial \mathbf{q}_u} & \frac{\partial \mathbf{r}_2}{\partial \mathbf{q}_v} & \mathbf{0} \\ \mathbf{0} & \frac{\partial \mathbf{r}_3}{\partial \mathbf{q}_v} & \frac{\partial \mathbf{r}_3}{\partial \mathbf{q}_p} \end{bmatrix} \quad (16)$$

**Remark 1** The discrete cost function  $\mathcal{J}$  defined by (10) is not differentiable due to the discontinuous Heaviside function  $H$ . If one wishes to use descent type optimization methods (and this will be our case), then smoothing of the Heaviside function is necessary (see Appendix 1) to make the components of the residual vector  $\mathbf{r}$  continuously differentiable functions of the design variables. Thus, while assembling the discrete system arising from  $(\mathcal{P}_\varepsilon^h(\psi))$ ,  $H$  will be replaced by a smoothed function  $H_\beta$ , i.e.  $G_\varepsilon = \frac{1}{\varepsilon} H_\beta$  in  $(\mathcal{P}_\varepsilon^h(\psi))$  in what follows.



**Remark 2** Notice that the equations are coupled in a quite complicated way. For example, the residual  $\mathbf{r}_1$  depends naturally on  $\mathbf{q}_u$ , but also on  $\mathbf{q}_v$  through the shapes of the elements as specified by (13). Moreover, since the mesh is moving and  $\psi$  is a function of location,  $\mathbf{r}_1$  depends on  $\mathbf{q}_v$  also through  $H_\beta(\psi)$ . This dependence must be taken into account especially during the sensitivity analysis phase in order to obtain perfectly consistent derivatives.

Despite this nonstandard coupling between the equations, the Jacobian matrix (16) is easy to compute using the sparse forward mode automatic differentiation [17]. Our implementation of the automatic differentiation technique is described in [18]. For a general introduction to the principles of automatic differentiation see [19].

If  $\mathcal{J}$  is smooth then using the well-known adjoint approach, the gradient  $\nabla_\alpha \mathcal{J}$  can be computed from

$$\nabla_\alpha \mathcal{J} = \left( \frac{\partial \mathbf{r}}{\partial \alpha} \right)^T \boldsymbol{\nu}, \quad (17)$$

where the adjoint vector  $\boldsymbol{\nu}$  solves the adjoint equation

$$\left( \frac{\partial \mathbf{r}}{\partial \mathbf{q}} \right)^T \boldsymbol{\nu} = -\nabla_{\mathbf{q}} \mathcal{J}. \quad (18)$$

The required Jacobian matrices and gradients in (17) and (18) can be again easily computed using the tools of automatic differentiation. Notice that the Jacobian  $\partial \mathbf{r} / \partial \alpha$  has a sparse structure, since the radial basis functions are compactly supported. This sparsity is automatically exploited, since we use the sparse forward mode automatic differentiation technique. To avoid going through all radial basis functions while evaluating  $\psi$ , a quadtree data structure is exploited to exclude RBFs that can not have a non-zero value at the point of evaluation.

## 4.5 Optimization strategy using remeshing

As explained in the previous paper [1], remeshing is sometimes needed since the mesh deformation approach can not handle too large displacements. Indeed, the Newton method used to solve the coupled system may not converge in case of excessive deformations of  $\hat{\Omega}$ . Moreover, if the mesh gets too distorted, significant errors in the solution and numerical instabilities may appear.

In this paper we adopt the following adaptive optimization strategy: to avoid too large deformation fields  $\mathbf{v}_h$  in  $(\mathcal{P}_\varepsilon^h(\psi))$  the reference domain  $\hat{\Omega}$  is re-initialized after  $k_{\max}$  optimization steps. Moreover, the half width  $\delta$  of the gray region related to the smoothing of the Heaviside function (see Appendix 1) is determined adaptively. This  $\delta$  is then used to determine the smoothing parameter  $\beta$ , i.e.  $\beta := \beta(\delta)$ . Note that due to this adaptive strategy  $\beta$  varies spatially, too. Therefore there are two smoothing parameters  $\varepsilon, \delta$  related to the discrete pseudo-solid problem which we thus denote by  $(\mathcal{P}_{\varepsilon, \delta}^h(\psi))$ .

The strategy of choosing  $\delta$  is also altered after  $k_{\max}$  optimization steps. In early steps a larger value of  $\delta$  is used, which makes the objective function smoother and enables fast progress. The value of  $\delta$  is then gradually decreased, improving the approximation of the exact Heaviside step function. We choose the half width  $\delta$  of the desired gray region after  $i$ :th re-initialization step to be

$$\delta = \frac{1}{2}(i_{\max} - i + 1)h, \quad (19)$$

where  $i_{\max}$  is the number of re-initializations to be done and  $h$  is the characteristic mesh size.

We choose the number of re-initializations to be modest, e.g.  $i_{\max} = 8$ . In the early stages of optimization the progress is rapid, and changes in the design domain  $\omega$  are large. Therefore we let the number of steps between re-initializations to increase in the course of optimization, e.g.  $k_{\max} = 5 \cdot 2^i$ .

The re-initialized optimization process can be described as the following algorithm:

**Algorithm 1** ( $i_{\max}, h, \text{toler}$  given)

Compute initial guess  $\alpha$  using eq. (12); (20)

Set  $\widehat{\Omega} := B(0, C(1, \gamma))$ ; (21)

**for**  $i = 1, \dots, i_{\max}$  (22)

Generate triangulation  $\widehat{\mathcal{T}}$  of  $\widehat{\Omega}$ ; (23)

Set  $\delta := \frac{1}{2}(i_{\max} - i + 1)h$  and  $k_{\max} = 5 \cdot 2^i$ ; (24)

**do** (25)

Set  $k := 1$ ; (26)

Solve state problem  $(\mathcal{P}_{\varepsilon, \delta}^h(\psi_N(\alpha)))$ ; (27)

Evaluate  $\mathcal{J}(\alpha)$  and  $\nabla_{\alpha} \mathcal{J}(\alpha)$  using (10), (17) and (18); (28)

Find descent direction  $\tilde{\alpha}$  of  $\mathcal{J}$  at  $\alpha$ ; (29)

Update design  $\alpha := \alpha + \tilde{\alpha}$ ; (30)

Set  $k := k + 1$ ; (31)

**while**  $k < k_{\max}$  and  $\|\tilde{\alpha}\| > \text{toler}$ ; (32)

Reinitialize  $\widehat{\Omega} := \Omega_{v_h}$  using the latest  $v_h$ ; (33)

**end** (34)

The re-initialization of  $\widehat{\Omega}$  in step (33) is done as follows. One fits by least squares a cubic B-spline curve to the outer boundary of the deformed mesh  $\mathcal{T}(v_h)$  obtained as the solution to the free boundary problem corresponding to the current design  $\alpha$ . Nodes are then distributed on this curve, and this geometry is given to the mesh generator Gmsh [20].

Thus, in algorithm (21)–(34) we basically solve  $i_{\max}$  different optimization problems, performing a mesh regeneration for each problem. The initial guess for the next problem is always the best design found so far, i.e. the end result of the previous problem.

## 5 Numerical examples

In this section we illustrate the performance of the proposed method. The target domains are the same as in [1]. The value of the penalty parameter  $\varepsilon$  is  $10^{-3}$ . We used the gradient based optimizer Donlp2 [21] to realize the step (29) in Algorithm 1. The parameters  $\alpha_{\min}, \alpha_{\max}$  were chosen as  $\pm 10^{20}$ , i.e. we have practically unconstrained minimization problem. The performed numerical computations indicated no need to pose more strict constraints.

**Example 1** The target  $\Gamma_t$  is the “rounded square”. The length of sides of the square is 4. Each corner is rounded using a quarter of a circle of radius 1. For the magnitude of the normal derivative the value  $\gamma = -1$  was used. It was observed in [1] that if the family  $\mathcal{O}$  of admissible inner inclusions contains only star-like domains  $\omega$ , then the target  $\Gamma_t$  can never be matched. Moreover, if the number of the design variables increased, the boundary  $\partial\omega$  became more and more oscillating.

The final reference domain  $\widehat{\Omega}$  was discretized using 18842 linear triangular elements. The number of RBFs used was  $30 \times 30$ . The initial value of the cost functional was 1.09. After 630 optimization steps (and 2376 function evaluations) the cost function reduced to the value  $3.78 \cdot 10^{-5}$ .

The final geometry and the contour plot of  $H_\beta(\psi_N^*)$  are shown in Figure 3.

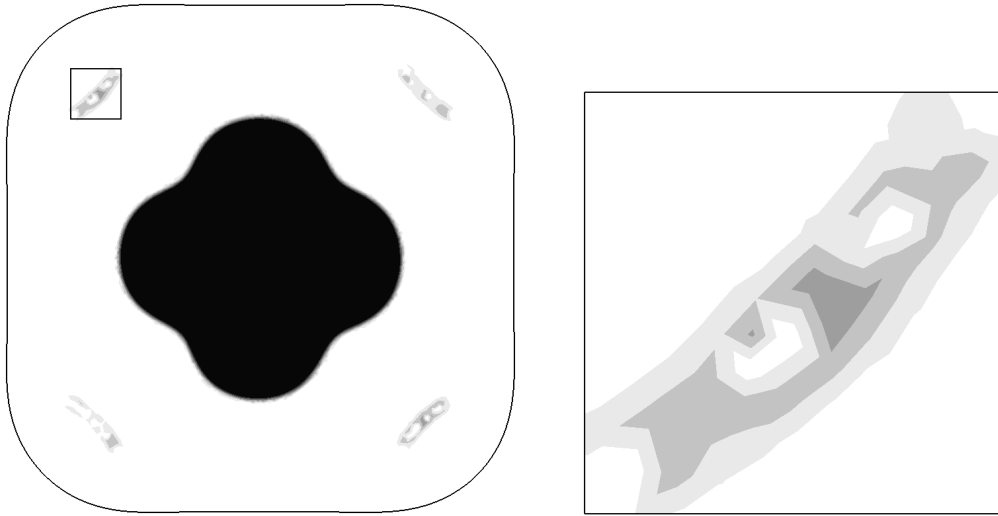


Figure 3: Left: the final geometry and  $H_\beta(\psi_N^*)$ . Right: zoom of the framed area.

In addition to “black” (i.e.  $\omega$ ) and “white” (i.e.  $\Omega \setminus \bar{\omega}$ ) regions, smoothing of the Heaviside function also produces by its construction “grey” regions (where  $0 < H_\beta(\psi_N^*) < 1$ ) near the zero level set of  $\psi$  representing  $\partial\omega$ . In the final design however grey regions which can not be interpreted as being close to  $\partial\omega$  may appear. In Figure 3 we see one of those problematic regions. By examining the potential  $u_h$  (see Figure 4) in that area, we find that the maximum value of  $u_h$  in this region is only about 0.86, whereas in  $\omega$  we should approximately meet the condition  $u_h = 1$ .

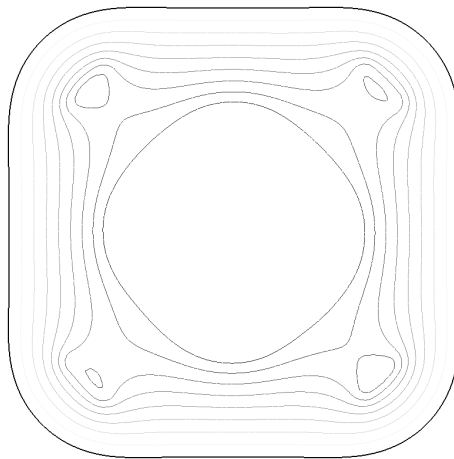


Figure 4: Contour plot of the potential  $u_h$  related to Example 1.

**Example 2** To prevent such problematic grey regions we propose to add the following penalty term to the cost functional  $\mathcal{J}$ :

$$\mathcal{J}_\eta = \eta \int_{\Omega} H_{2\beta}(\psi)(u - 1)^2 dx, \quad \eta > 0. \quad (35)$$

The idea behind is the following. The penalty  $\mathcal{J}_\eta$  will be zero where  $H_{2\beta}$  is zero or  $u = 1$  is met. Near the boundary of  $\omega$  the solution  $u$  is close to 1, and  $\mathcal{J}_\eta$  is small. However, in regions like the one shown in Figure 3 the value of  $\mathcal{J}_\eta$  is larger since  $u_h$  is much less than 1. Notice that instead of the original value used in the state problem, a two times larger value  $2\beta$  was used in the smoothing of the Heaviside function in (35).

This approach turns out to be effective. In Figures 5 and 6 we show the results for the same problem as in Example 1 but with the penalty term included. The value of the penalty parameter was  $\eta = 0.1$ . Now the problematic grey regions near the corners have disappeared, and have been replaced by regions where the Heaviside function has the value  $H_\beta = 1$ . Also the potential  $u_h$  is close to 1 near this region (see Figure 6). This time the optimizer needed 1009 iterations and 4098 function evaluations. The final values are  $\mathcal{J} = 7.67 \cdot 10^{-5}$  and  $\mathcal{J}_\eta = 8.42 \cdot 10^{-5}$ .



Figure 5: The final geometry and  $H_\beta(\psi_N^*)$ .

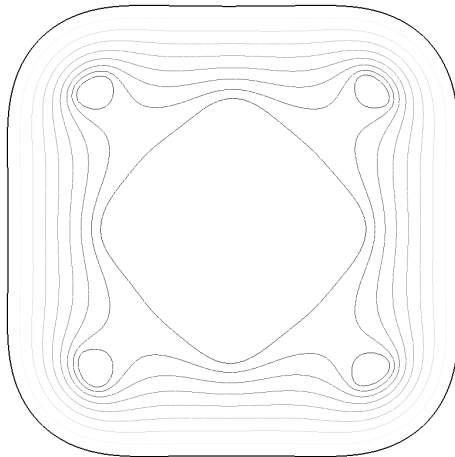


Figure 6: The potential  $u_h$  related to Example 2.

**Example 3** Let  $\gamma = -2$  and let the radius function defining the target boundary  $\Gamma_t$  be chosen as follows:

$$g_t(\theta) = 0.5 \cos(\theta) + 0.8 \cos(2\theta) + 2, \quad \theta \in [0, 2\pi[.$$

The final finite element mesh consists of 15820 linear triangular elements, and the number of RBFs is  $15 \times 15$ . Value of the penalty parameter was  $\eta = 0.01$ . The initial value of the objective function (i.e. the sum of  $\mathcal{J}$  and  $\mathcal{J}_\eta$ ) was 4.77. After the total of 356 optimization steps and 1559 function evaluations this value was reduced to  $1.90 \cdot 10^{-5}$ . The results of computations are depicted in Figures 7 and 8.

This problem was solved in [1] using a fixed topology approach. The results of computations led to a conclusion that the inner boundary consists of more than one component. From this reason two holes as an initial approximation of the inner boundary were introduced “by hand”, each parameterized by the radial co-ordinates. The obtained result was similar to that in Figure 7.

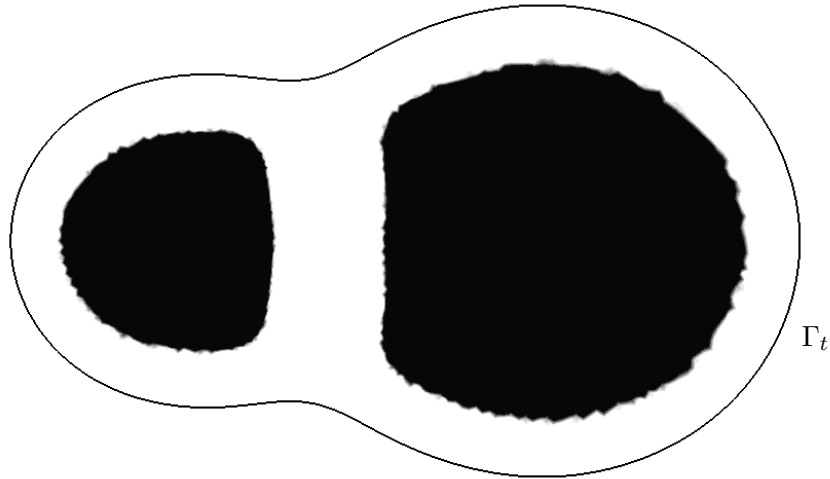


Figure 7: The final geometry and  $H_\beta(\psi_N^*)$

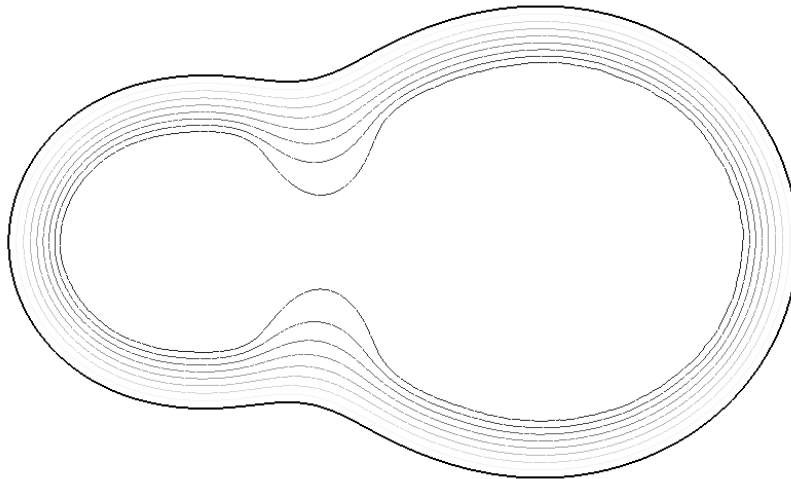


Figure 8: The potential  $u_h$  related to Example 3.

## 6 Conclusions

In this paper we have considered topology optimization with the state constraint given by a free boundary problem of Bernoulli type. To solve efficiently the free boundary problems during the optimization, the pseudo-solid approach is applied. Its main advantage is that there is no explicit parametrization of the shape of the free boundary using e.g. splines. The novelty of the numerical method proposed in this paper is the combination of the pseudo-solid approach to tackle the free boundary problem with a parameterized level set method for shape optimization. It has been found already in [1] that the problem is very badly conditioned as many different choices of  $\omega$  may lead to nearly identical free boundaries. Therefore the progress of the optimization is often slow. The proposed method can be applied in an analogous way to topology optimization problems governed by other free boundary problems.

## References

- [1] J. I. Toivanen, J. Haslinger, and R. A. E. Mäkinen, “Shape optimization of systems governed by Bernoulli free boundary problems,” *Computer Methods in Applied Mechanics and Engineering*, vol. 197, pp. 3803–3815, 2008.
- [2] M. Flucher and M. Rumpf, “Bernoulli’s free boundary problem, qualitative theory and numerical approximation,” *J. Reine Angew. Math.*, vol. 486, pp. 165–204, 1997.
- [3] K. Kärkkäinen and T. Tiihonen, “Free surfaces: shape sensitivity analysis and numerical methods,” *International Journal for Numerical Methods in Engineering*, vol. 44, no. 8, pp. 1079–1098, 1999.
- [4] C. Cuvelier and R. M. S. M. Schulkes, “Some numerical methods for the computation of capillary free boundaries governed by the Navier-Stokes equations,” *SIAM Review*, vol. 32, no. 3, pp. 355–423, 1990.
- [5] J. Haslinger and R. A. E. Mäkinen, *Introduction to Shape Optimization: Theory, Approximation, and Computation*. SIAM, Philadelphia, 2003.
- [6] R. A. Cairncross, P. R. Schunk, T. A. Baer, R. R. Rao, and P. A. Sackinger, “A finite element method for free surface flows of incompressible fluids in three dimensions. Part I. Boundary fitted mesh motion,” *International Journal for Numerical Methods in Fluids*, vol. 33, pp. 375–403, 2000.
- [7] M. Souli and J. P. Zolesio, “Arbitrary Lagrangian-Eulerian and free surface methods in fluid mechanics,” *Computer Methods in Applied Mechanics and Engineering*, vol. 191, pp. 451–466, 2001.
- [8] S. Osher and J. A. Sethian, “Fronts propagating with curvature dependent speed: Algorithms based on Hamilton-Jacobi formulations,” *Journal of Computational Physics*, vol. 79, pp. 12–49, 1988.
- [9] S. Osher and R. Fedkiw, *Level Set Methods and Dynamic Implicit Surfaces*. Springer Verlag, 2003.
- [10] G. Allaire, F. Jouve, and A.-M. Toader, “Structural optimization using sensitivity analysis and level-set methods,” *Journal of Computational Physics*, vol. 194, pp. 363–393, 2004.

- [11] S. Wang and M. Y. Wang, “Radial basis functions and level set method for structural topology optimization,” *International Journal for Numerical Methods in Engineering*, vol. 65, pp. 2060–2090, 2006.
- [12] J. Chen, V. Shapiro, K. Suresh, and I. Tsukanov, “Shape optimization with topological changes and parametric control,” *International Journal for Numerical Methods in Engineering*, vol. 71, no. 3, pp. 313–346, 2007.
- [13] T. Belytschko, S. P. Xiao, and C. Parimi, “Topology optimization with implicit functions and regularization,” *International Journal for Numerical Methods in Engineering*, vol. 57, pp. 1177–1196, 2003.
- [14] P. Neittaanmäki, A. Pennanen, and D. Tiba, “Fixed domain approaches in shape optimization problems with Dirichlet boundary conditions,” *Inverse Problems*, vol. 25, no. 5, 2009. Article number 055003 (18pp).
- [15] Z. Luo, M. Y. Wang, S. Wang, and P. Wei, “A level set-based parameterization method for structural shape and topology optimization,” *International Journal for Numerical Methods in Engineering*, vol. 76, pp. 1–26, 2008. DOI: 10.1002/nme.2092.
- [16] H. Wendland, “Piecewise polynomial, positive definite and compactly supported radial functions of minimal degree,” *Advances in Computational Mathematics*, vol. 4, no. 1, pp. 389–396, 2005.
- [17] C. H. Bischof, P. M. Khademi, A. Bouaricha, and A. Carle, “Efficient computation of gradients and Jacobians by dynamic exploitation of sparsity in automatic differentiation,” *Optimization Methods and Software*, vol. 7, pp. 1–39, 1996.
- [18] J. I. Toivanen and R. A. E. Mäkinen, “Implementation of sparse forward mode automatic differentiation with application to electromagnetic shape optimization,” *Optimization Methods and Software*, 2010. To appear, published online.
- [19] A. Griewank and A. Walther, *Evaluating Derivatives: Principles and Techniques of Algorithmic Differentiation*. SIAM, Philadelphia, 2nd ed., 2008.
- [20] C. Geuzaine and J.-F. Remacle, “Gmsh: A 3-D finite element mesh generator with built-in pre- and post-processing facilities,” *International Journal for Numerical Methods in Engineering*, vol. 79, pp. 1309 – 1331, 2009.
- [21] P. Spellucci, “An SQP method for general nonlinear programs using only equality constrained subproblems,” *Mathematical Programming*, vol. 82, pp. 413–448, 1998. Software available at <http://plato.la.asu.edu/donlp2.html>.

## Appendix 1

### Smoothing the Heaviside function

The expression for the  $C^2$ -smoothed Heaviside function is done by

$$H_{\beta}(y) = \begin{cases} 0, & \text{if } y < -\beta \\ 1, & \text{if } y > \beta \\ \left(\frac{y}{\beta} - \frac{y^3}{3\beta^3}\right) \frac{3}{4} + \frac{1}{2} & \text{otherwise,} \end{cases} \quad (36)$$

where  $\beta > 0$  is a given constant.

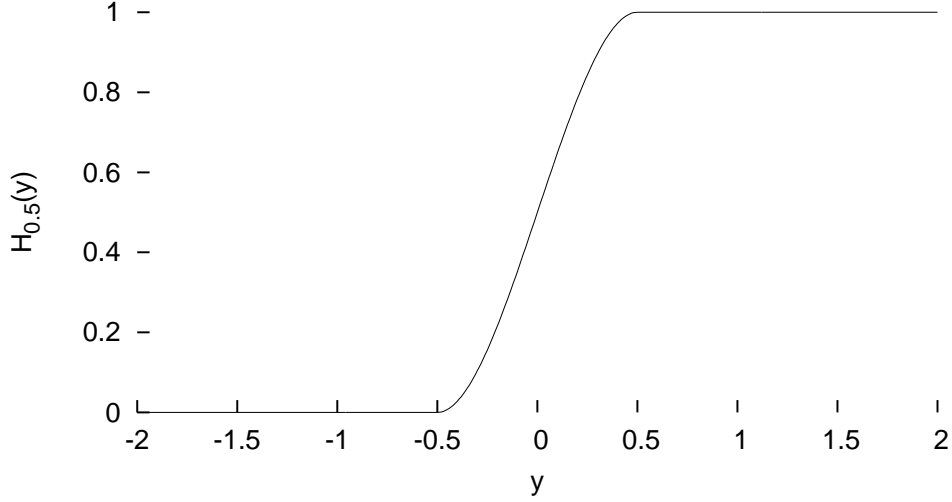


Figure 9: The graph of  $H_\beta$ ,  $\beta = \frac{1}{2}$ .

If  $\psi(\mathbf{x}) \in ]-\beta, \beta[$  then  $\mathbf{x}$  belongs to the so-called grey region, i.e.  $H_\beta(\psi(\mathbf{x})) \in ]0, 1[$ . Such regions appear near the boundaries of the design domain  $\omega$ . To maintain a good quality of the gradients that we obtain, we would like to have the geometrical width of the grey region to be approximately constant everywhere. If the scalar function  $\psi$  approximated the signed distance function, this would automatically be the case. However, we do not make this requirement, but instead we propose the following procedure.

Let  $2\delta$  be the desired width of the grey region. Consider a point  $\mathbf{x}_0$  on the zero level set, and a point  $\mathbf{x}$  located at  $\mathbf{x} = \mathbf{x}_0 + \delta\mathbf{n}$ , where  $\mathbf{n}$  is the unit normal vector to the zero level set of  $\psi$ . The unit normal vector is  $\mathbf{n} = \nabla\psi/\|\nabla\psi\|$ , thus we can write

$$\mathbf{x} = \mathbf{x}_0 + \delta\mathbf{n} = \mathbf{x}_0 + \delta \frac{\nabla\psi(\mathbf{x}_0)}{\|\nabla\psi(\mathbf{x}_0)\|}. \quad (37)$$

Since on the other hand we have the first order approximation

$$\psi(\mathbf{x}) \approx \psi(\mathbf{x}_0) + (\mathbf{x} - \mathbf{x}_0) \cdot \nabla\psi(\mathbf{x}_0), \quad (38)$$

we get from (37) and (38) that

$$\psi(\mathbf{x}) - \psi(\mathbf{x}_0) \approx \delta \frac{\nabla\psi(\mathbf{x}_0)}{\|\nabla\psi(\mathbf{x}_0)\|} \cdot \nabla\psi(\mathbf{x}_0) = \delta\|\nabla\psi(\mathbf{x}_0)\| \quad (39)$$

Thus if we use

$$\beta(\mathbf{x}) = \delta\|\nabla\psi(\mathbf{x})\| + 10^{-6} \quad (40)$$

as the Heaviside parameter, the width of the grey region will be approximately  $2\delta$  everywhere. The constant  $10^{-6}$  is added to prevent division by zero, since  $\beta$  appears in the denominator in (36).



## Appendix 2

### Analytical solution in the circular domain

Let  $\omega = B(0, R)$ , where  $B(0, R)$  is the circle of radius  $R$  centered at the origin, and  $C := C(R, \gamma)$  be a constant such that

$$C \ln(C) - C \ln(R) = -\frac{1}{\gamma}, \quad \gamma < 0. \quad (41)$$

The function

$$f(R, \gamma) := C\gamma \ln(\sqrt{x^2 + y^2}) - C\gamma \ln(R) + 1 \quad (42)$$

satisfies  $\Delta f = 0$  in  $\Omega \setminus \bar{\omega}$ ,  $f = 1$  on  $\partial\omega$  and  $\nabla f \cdot \mathbf{n} = \gamma$  on  $\partial B(0, C(R, \gamma))$ . Thus, given  $\gamma < 0$  and  $\omega = B(0, R)$ , we know that the analytical solution of the free boundary problem  $(\tilde{\mathcal{P}}(\omega))$  is  $u = f(R, \gamma)$  and  $\Omega = B(0, C(R, \gamma))$ . Finally, a level set function representing  $B(0, R)$  is given by

$$\hat{\psi}_R(x, y) = R - \sqrt{x^2 + y^2}. \quad (43)$$